Cornell University
Laboratory for Elementary-Particle Physics

USPAS course on

Recirculated and Energy Recovered Linacs

Ivan Bazarov, Cornell University

Geoff Krafft, JLAB

Electron Sources: Space Charge in Injectors

Jefferson Lab

Contents

- Space charge
- Debye length
- Equilibrium distribution
- Beam envelope equation
- Emittance compensation
- Computational aspects
- Optimal initial pulse distribution

Space charge

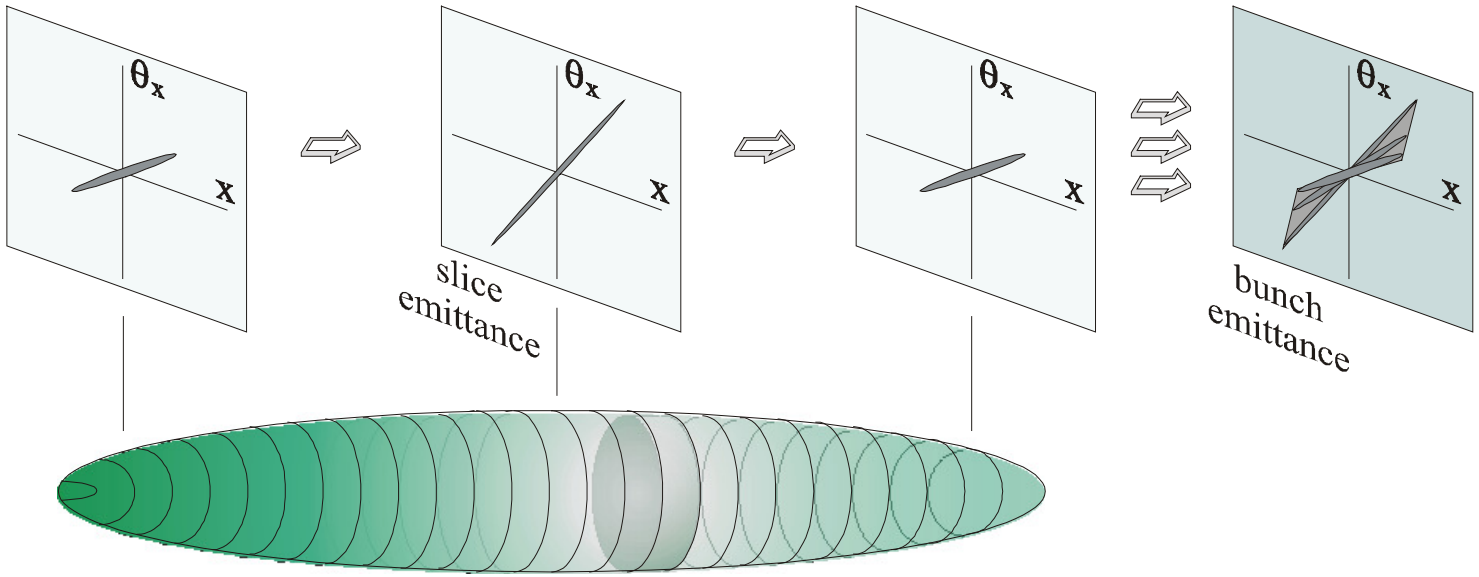

In a typical bunched beam from a gun, both charge and current density are functions of transverse & longitudinal coordinates. This makes space charge dominated behavior highly nonlinear.

For beam envelope equation we will assume that ρ and J_z are independent of transverse coordinate and that the beam is not bunched (aspect ration << 1).

"Collisional" vs. "smooth" self-fields

It would seem that the easiest approach is to calculate Lorentz force of all electrons directly (this would encompass practically *all* the behavior of the beam). This is not feasible because the number of evaluations for each time step is ~ N^2, with N ~ 10^{10}. Taking the fastest supercomputer with 100 TFLOPS, one estimates ~ year(s) per time step (and one may need something like ~10^4 steps).

Instead, people use macroparticles in computer simulations with the same *e/m* ratio

When N $\rightarrow \infty$ forces are smooth; when N $\rightarrow$ 1 grainy collisional forces dominate. Envelope equation assumes the first scenario.

How to determine quantitatively "collisional" vs. "smooth" behavior of the space charge in the beam?

Debye length and plasma frequency

Three characteristic lengths in the bunch:

a bunch dimension; l_p interparticle distance; λ_D Debye length

Interactions due to Coulomb forces are long-range; Debye length is a measure of how 'long' (screen-off distance of a local perturbation in charge).

for nonrelativistic case:

$$\omega_p = \sqrt{\frac{e^2 n}{\varepsilon_0 m}}, \sigma_{v_x} = \sqrt{\frac{k_B T}{m}}$$

$$\lambda_D = \sqrt{\frac{\varepsilon_0 k_B T}{e^2 n}}$$

$$\lambda_D \equiv \frac{\sigma_{v_x}}{\omega_p}$$

for relativistic case:

$$\omega_p = \sqrt{\frac{e^2 n}{\varepsilon_0 m \gamma^3}} \quad \sigma_{v_x} = \sqrt{\frac{k_B T}{m\gamma}}$$

$$\lambda_D = \sqrt{\frac{\gamma^2 \varepsilon_0 k_B T}{e^2 n}}$$

Debye length: beam dynamics scenarios

$\lambda_D >> a$ — YES → single-particle behavior dominates; true when either energy or beam temperature is large (emittance-dominated)

NO

collective forces are important

$$\varepsilon_n \sim \frac{\sigma_x \sigma_{p_x}}{mc} = \frac{\gamma \sigma_x \sigma_{v_x}}{c} = const$$

$$\gamma \sigma_x^2 k_B T = const$$

$\lambda_D >> l_p$ — YES → "smooth" force; Liouville's theorem can be defined in 6-D phase space; **if** forces are linear rms emittance is also conserved

NO

fields of individual particles become important; one ends up having 6N-D phase space to deal with in the worst case; beam tends to develop 'structure'

Equilibrium distribution

Similar to thermodynamics and plasma physics, there may exist equilibrium particle distributions (i.e. those that remain stationary). Vlasov theory allows one to find such distributions (assumes collisions are negligible, but they are the ones responsible to drive the distribution to the equilibrium!). Without the derivation, Vlasov-Maxwell equations for equilibrium distributions $f(q_i,p_i,t)$ (i.e. no explicit time dependence, $\partial/\partial t = 0$):

$$\sum_{i=1}^{3}\left[\frac{\partial f}{\partial q_i}\dot{q}_i + e(\vec{E}+\vec{v}\times\vec{B})_i\frac{\partial f}{\partial p_i}\right]=0$$

$$\vec{\nabla}\times\vec{E}=0 \qquad \vec{\nabla}\cdot\vec{E}=\frac{e}{\varepsilon_0}\int f\,d^3p$$

$$\vec{\nabla}\times\vec{B}=\mu_0 e\int \vec{v}f\,d^3p \qquad \vec{\nabla}\cdot\vec{B}=0$$

Equilibrium distribution (contd.)

In particular, in a constant focusing channel, equilibrium transverse density obeys a well-known Boltzmann relation

$$n(r) = n(0)\exp\left[-\frac{e\phi(r)}{k_B T_\perp}\right]$$

$$\phi(r) = \phi_{ext}(r) + \frac{1}{\gamma^2}\phi_{self}(r)$$

$$e\phi_{ext}(r) = \gamma m\omega_0^2 r^2/2$$

$$\varphi_{self}(r) = -\int_0^r\int_0^{\hat{r}} dr d\hat{r}\left(\frac{e}{\varepsilon_0 r}\hat{r}n(\hat{r})\right)$$

Equilibrium distribution (contd.)

Analytically, two extreme cases:

$$k_B T \to 0 \quad (\lambda_D / a \to 0) \qquad n(r) = \begin{cases} n_0 = const, \text{ for } r \le a \\ 0, \text{ for } r > a \end{cases} \qquad \textit{uniform}$$

$$\varphi_{self} \to 0 \quad (\lambda_D / a \ge 1) \qquad n(r) = n_0 \exp\left[-\frac{\gamma m \omega_0^2 r^2}{2 k_B T_\perp} \right] \qquad \textit{Gaussian}$$

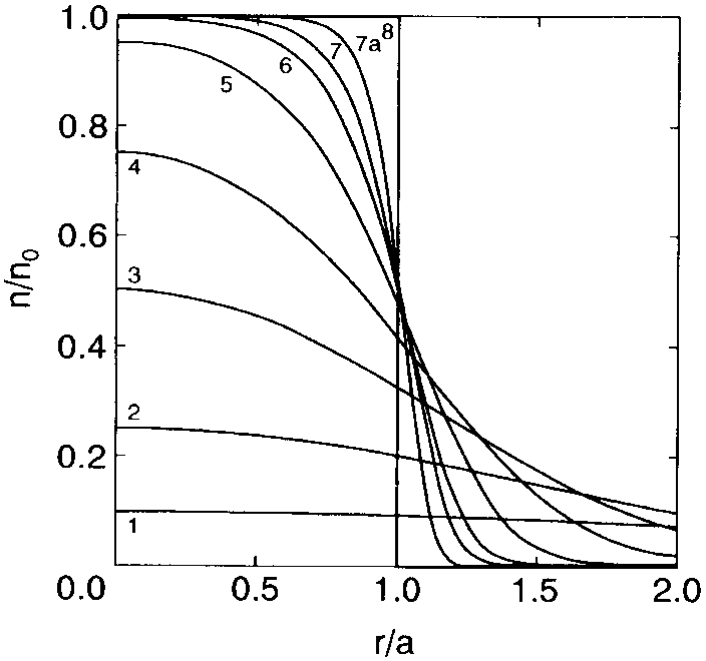

Curve	$n(0)/n_0$	$\lambda_D(0)/a_0$	Ka^2/ϵ^2
1	0.1	4.82	0.054
2	0.25	1.81	0.153
3	0.5	0.795	0.396
4	0.75	0.432	0.893
5	0.95	0.229	2.51
6	0.995	0.145	6.00
7	0.9995	0.107	10.9
7a	0.999995	0.0710	24.8
8	1	0	∞

Perveance and characteristic current

Let's derive beam envelope equation (i.e. we assume that self-forces are smooth). We have almost derived the equation already (previous lecture's paraxial ray equation). Two terms are missing – due to space charge and emittance 'pressure'.

Uniform laminar beam in the absence of external forces:

$$\gamma m\ddot{r} = \frac{eIr}{2\pi\varepsilon_0 a^2 \beta c}\frac{1}{\gamma^2}, \text{ using } \ddot{r} = \beta^2\gamma^2 r'' \rightarrow r'' = \frac{eIr}{2\pi\varepsilon_0 a^2 mc^3 \beta^3\gamma^3}$$

$$\ddot{r} = \frac{\omega_p^2}{2} r \qquad r'' = \frac{K}{a^2} r \qquad r_m r_m'' = K \quad \text{for } r_m = a$$

$$\omega_p^2 = \frac{eI}{\pi\varepsilon_0 mc\beta\gamma^3 a^2} \qquad K = \frac{I}{I_0}\frac{2}{\beta^3\gamma^3} \qquad I_0 = \frac{4\pi\varepsilon_0 mc^3}{e} \approx \frac{1}{30}\frac{mc^2}{e} = 17\text{kA}$$

Emittance 'pressure' term

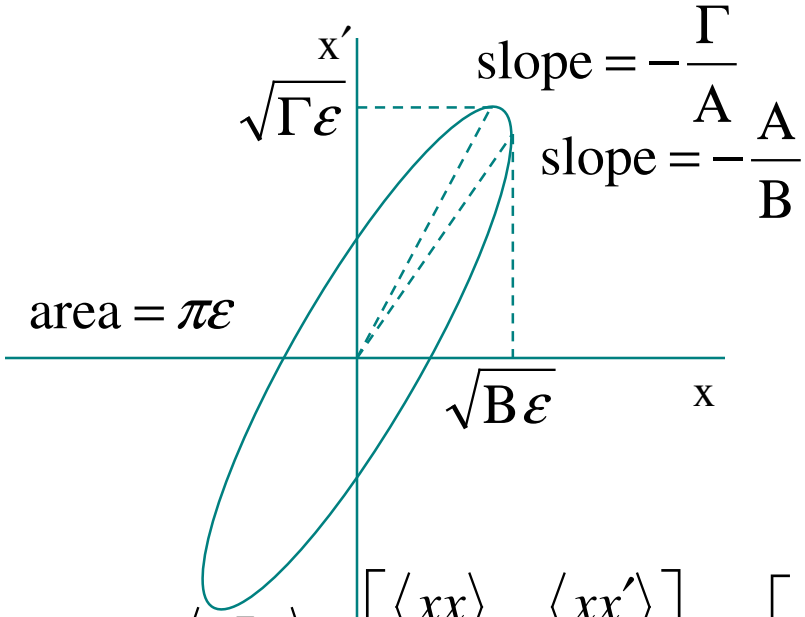

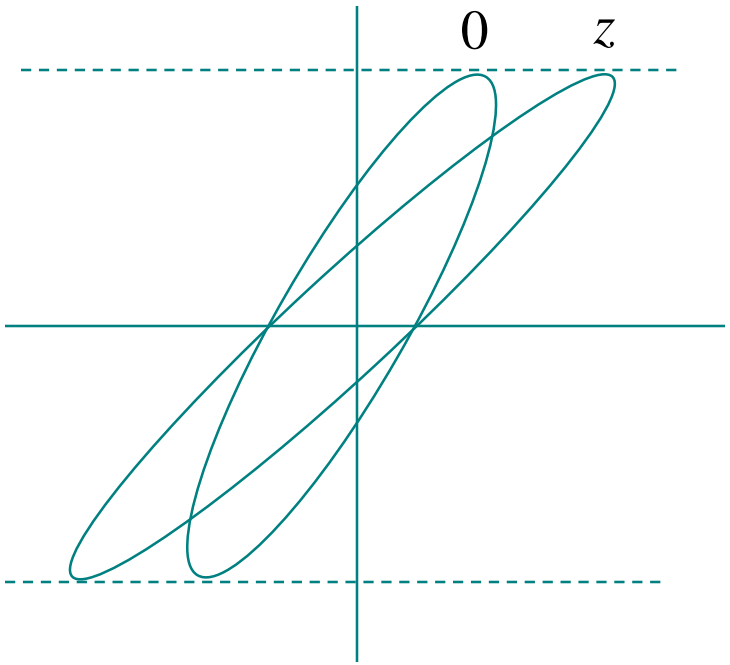

$$\det[\ldots] = 1$$

$$\Sigma = \left\langle \vec{x}^T \vec{x} \right\rangle = \begin{bmatrix} \langle xx \rangle & \langle xx' \rangle \\ \langle x'x \rangle & \langle x'x' \rangle \end{bmatrix} = \varepsilon \begin{bmatrix} B & -A \\ -A & \Gamma \end{bmatrix}$$

In a drift $0 \rightarrow z$: $\quad x' \rightarrow x' = const$, $\quad x \rightarrow x + x'z$ $\quad$ and $\quad B \rightarrow B - 2Az + \Gamma z^2$, $\quad A \rightarrow A - \Gamma z$, $\quad \Gamma \rightarrow \Gamma = const$

For σ_x: $\quad \sigma_x' = -\frac{\sqrt{\varepsilon}A}{\sqrt{B}}$, $\quad \sigma_x'' = \frac{\sqrt{\varepsilon}}{B\sqrt{B}}$ $\quad$ or $\quad \boxed{\sigma_x'' - \frac{\varepsilon^2}{\sigma_x^3} = 0}$

Beam envelope equation

From paraxial ray equation with the additional terms, one obtains

$$\sigma'' + \sigma' \frac{\gamma'}{\beta^2\gamma} + \sigma \frac{1}{\beta^2\gamma^2}\left[\frac{\gamma''\gamma}{2} + \left(\frac{eB}{2mc}\right)^2\right] - \frac{1}{\sigma}\frac{I}{2I_0\beta^3\gamma^3} - \frac{1}{\sigma^3}\frac{1}{\beta^2\gamma^2}\left[\left(\frac{P_\theta}{mc}\right)^2 + \varepsilon_n^2\right] = 0$$

adiabatic

RF focusing of cavity edge

solenoid

space charge

angular momentum 'increases' emittance

$$\frac{I}{2I_0\beta\gamma} >> \frac{\varepsilon_n^2}{\sigma^2}, \text{ or } \frac{I}{2I_0\beta^2\gamma^2} >> \frac{\varepsilon_n}{\mathrm{B}}$$

space charge dominated

$$\frac{I}{2I_0\beta\gamma} << \frac{\varepsilon_n^2}{\sigma^2}, \text{ or } \frac{I}{2I_0\beta^2\gamma^2} << \frac{\varepsilon_n}{\mathrm{B}}$$

emittance dominated

Emittance evolution due to space charge

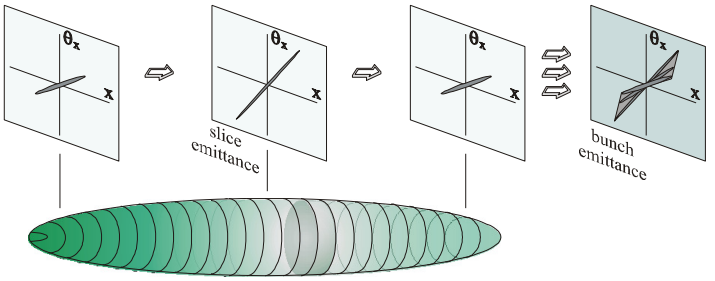

We have seen that beam will evolve from space-charge dominated to emittance dominated regimes as it is being accelerated. At low energies, various longitudinal 'slices' of the bunch experience different forces due to varying current → 'bow-tie' phase space is common.

Important realization is that much of these space charge emittance growth may be reversible through appropriate focusing (and drifts), a so-called emittance compensation. Obviously, this emittance compensation should take place before (or rather as) the beam becomes ultrarelativistic (and emittance-dominated).

Emittance growth in RF guns (without comp.)

Kim analyzed emittance growth due to space charge and RF (NIM A **275** (1989) 201-218). His analysis applies to beam in RF guns. He has found:

$$\varepsilon_x^{rf} = \frac{\alpha k_{RF}^3 \sigma_x^2 \sigma_z^2}{\sqrt{2}} \qquad \boxed{\alpha \downarrow}$$

$$\alpha = \frac{eE_0}{2mc^2 k_{RF}}$$

$$\varepsilon_x^{sc} = \frac{\pi}{4} \frac{1}{\alpha k_{RF}} \frac{1}{\sin\phi_0} \frac{I_{peak}}{I_0} \mu_x(A) \qquad \boxed{\alpha \uparrow}$$

$$\mu_{x,gauss} \approx \frac{1}{3A+5}$$

e.g. 100 MV/m RF gun (λ = 10.5 cm): α = 1.64, phase (to minimize rf emittance) ϕ_0 = 71° ($\phi \rightarrow$ 90°), laser width and length σ_x = 3.5 mm, σ_z = 0.6 mm

$$\varepsilon_x^{rf} = 1.1\,\text{mm - mrad}$$

$$\varepsilon_x^{sc} = 4.0\,\text{mm - mrad (1.3 mm - mrad for uniform)}$$

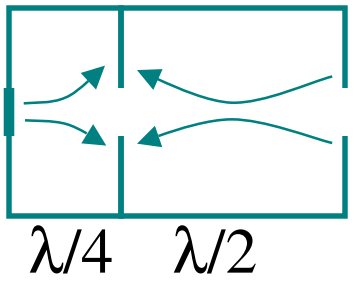

Emittance Compensation

Carlsten noted in simulations that emittance can be brought down and gave a simple explanation for the effect (NIM A **285** (1989) 313-319).

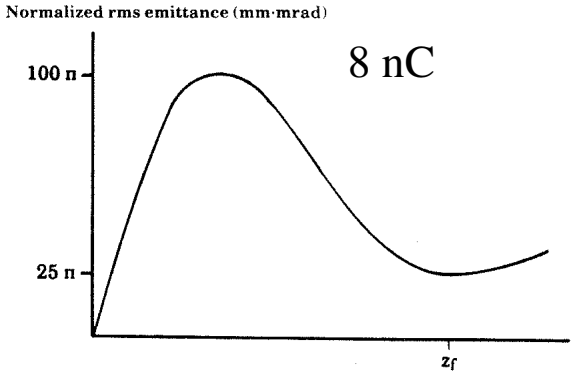

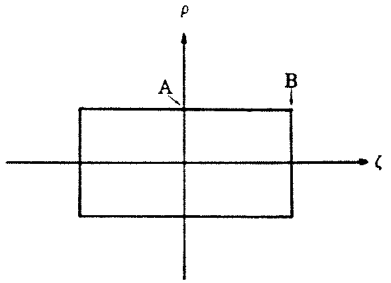

Fig. 2. Typical transverse emittance versus beamline position plot for a photoelectric injector, showing quick initial growth and subsequent reduction for a slug beam and physical description of a slug beam, with internal coordinates ρ and ζ.

5. Conclusion

A photoelectric injector design analysis has been presented. The emittance growth from the dominant mechanism has been shown to be eliminated with a simple lens configuration, leaving only a small residual emittance resulting from the other mechanisms.

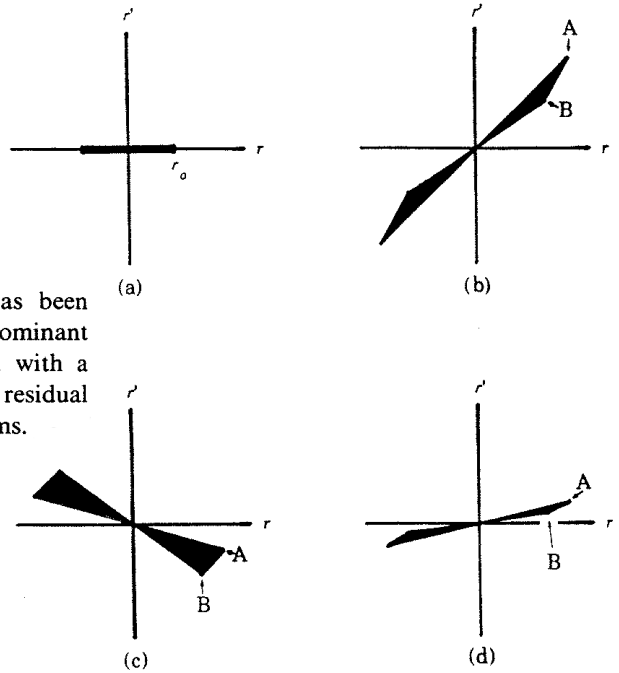

Fig. 3. Transverse phase-space plots showing emittance growth and reduction. (a) Initial phase-space plot with very small emittance. (b) Phase space plot after drift z_1 to lens, showing the emittance growth due to the different expansion rates of points A and B. (c) Phase-space plot immediately after lens, showing rotation due to the lens. The emittance is unchanged because we assume the lens is linear. (d) Phase space plot after drift z behind lens, showing the emittance reduction due to the different expansion rates of points A and B.

Emittance compensation from envelope eqn.

Serafini and Rosenzweig used envelope equation to explain emittance compensation (Phys. Rev. E **55** (1997) 7565).

$$\sigma'' + \sigma' \frac{\gamma'}{\beta^2\gamma} + \sigma K_r - \frac{I(\zeta)}{\sigma 2 I_0 \beta^3 \gamma^3} - \frac{\varepsilon_n^2}{\sigma^3 \beta^2 \gamma^2} = 0$$

includes solenoid and RF

ζ tags long. slice in the bunch

For space charge dominated case in absence of acceleration

$$\sigma'' + \sigma' \frac{\gamma'}{\beta^2\gamma} + \sigma K_r - \frac{I(\zeta)}{2\sigma I_0 \beta^3 \gamma^3} - \frac{\varepsilon_n^2}{\sigma^3 \beta^2 \gamma^2} = 0$$

Brillouin flow $\sigma'' \to 0$:

$$\sigma_{eq} = \sqrt{\frac{I(\zeta)}{2 K_r I_0 \beta^3 \gamma^3}}$$

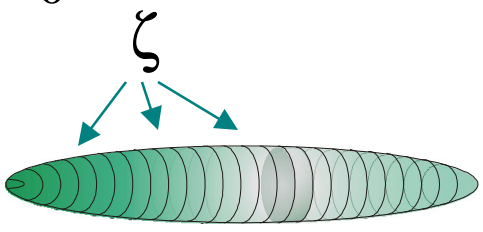

Emittance compensation

Small oscillations near equilibrium: $\delta\sigma'' + \delta\sigma\left[2K_r - \frac{\delta\sigma}{\sigma_{eq}} + \left(\frac{\delta\sigma}{\sigma_{eq}}\right)^2 - \ldots\right] = 0$ (the $\frac{\delta\sigma}{\sigma_{eq}}$ term is marked 0)

Important: frequency of small oscillations around equilibrium does not depend on ζ. E.g. for beam with $\sigma'(0,\zeta) = 0$ and $\sigma(0,\zeta) = \sigma_{eq}(\zeta) + \delta\sigma(\zeta) = \sigma_0$:

$$\begin{cases} \sigma(z,\zeta) = \sigma_{eq}(\zeta) + \delta\sigma(\zeta)\cos\left(\sqrt{2K_r}\,z\right) \\ \sigma'(z,\zeta) = -\sqrt{2K_r}\,\delta\sigma(\zeta)\sin\left(\sqrt{2K_r}\,z\right) \end{cases}$$

$$\varepsilon = \frac{1}{2}\sqrt{\left\langle r^2\right\rangle\left\langle r'^2\right\rangle - \left\langle r'r\right\rangle^2} \approx \sqrt{2K_r}\left\langle\sigma_{eq}\right\rangle\sigma_0\left|\sin(\sqrt{2K_r}\,z)\right|$$

Emittance compensation

- slices oscillate in phase space around different equilibria but with the same frequency
- 'projected' emittance reversible oscillations when $\delta\sigma/\sigma_{eq} << 1$, unharmonicity shows up when $\delta\sigma$ is not small
- ignores the fact that beam aspect ratio can be >> 1 (e.g. at the cathode)

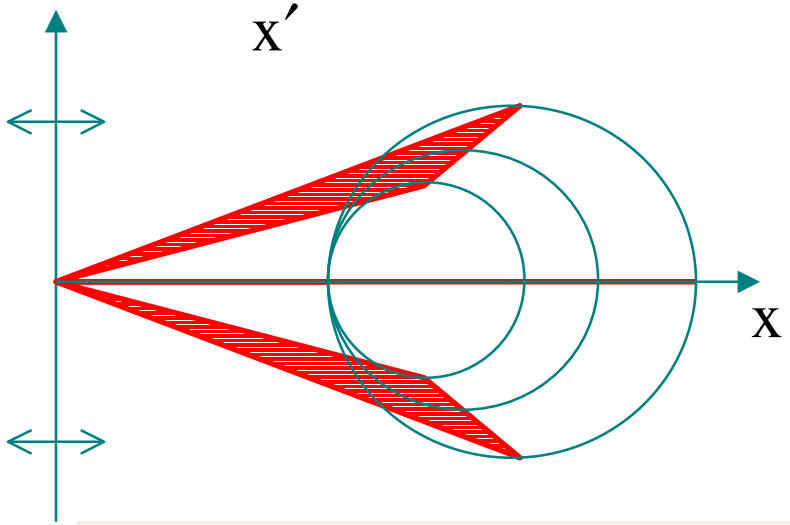

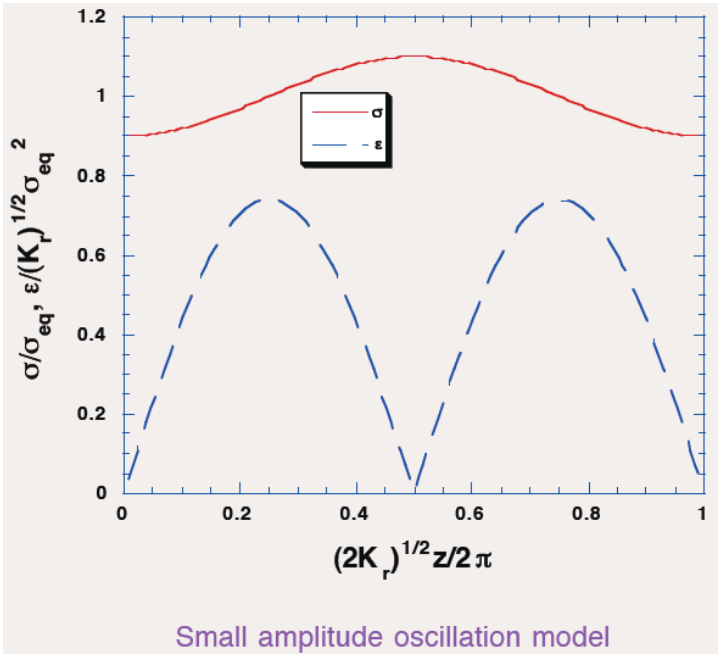

Small amplitude oscillation model

Emittance compensation

Including acceleration term and transforming from (σ,z) → (τ,y) in the limit γ >> 1

$$\frac{d^2\tau}{dy^2} + \Omega^2\tau = \frac{e^{-y}}{\tau}$$

$y \equiv \ln\frac{\gamma}{\gamma_0}, \tau \equiv \sigma\gamma'\sqrt{\gamma_0/(I(\zeta)/2I_0)}$, Ω represents solenoid & RF focusing

Particular solution that represents generalized Brillouin flow or 'invariant envelope':

$$\tau_{eq} = \frac{2e^{-y/2}}{\sqrt{1+4\Omega^2}}, \sigma_{eq} = \frac{2}{\gamma'}\sqrt{\frac{I(\zeta)}{\gamma 2I_0}\frac{1}{1+4\Omega^2}}$$

$\frac{\gamma\sigma'_{eq}}{\sigma_{eq}} = -\frac{\gamma'}{2}$ phase space angle is independent of slice ζ

Matching beam to 'invariant envelope' can lead to 'damping' of projected rms emittance.

Numerical approach

Using the beam envelope equation for individual slices leads to a recipe for emittance compensation, which works for simple cases (e.g. matching beam into long focusing channel / linac in the injector). For other more complicated scenarios one should solve the equations numerically (example: code HOMDYN).

Finally, particle tracking is indispensable for analysis and design of the injector where the assumptions made are invalid or theory is too complicated to be useful.

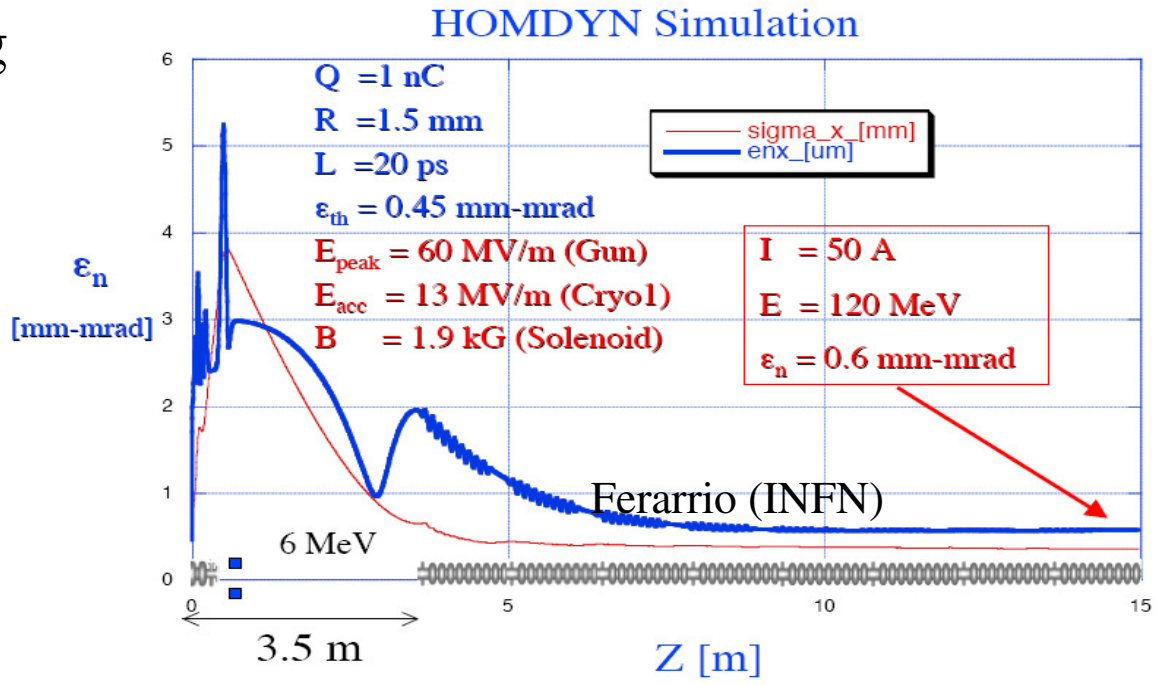

Computer Modeling

- It used to be the case that extensive modeling of the injector was too demanding in terms of time & computer resources to allow finding optima for generating bright beams by varying more than a couple (or so) parameters.
- This is no longer true. Advances in space charge codes & computing abilities allow extensive study / optimization of nonlinear space charge problem in the injector with good precision and minimal number of assumptions.
- Numerical studies can give insights and better understanding of beam dynamics in the injector.

Space charge codes

Different approaches are used (e.g. envelope equation integration, macroparticle tracking, various meshing scenarios, etc.).
Mesh method works as following:

1) transform to rest frame of the reference particle
2) create mesh (charge) and cell grid (electrostatic fields)
3) create table containing values of electrostatic field at any cell due to a unit charge at any mesh vertex (does not need to be recalculated each time step)

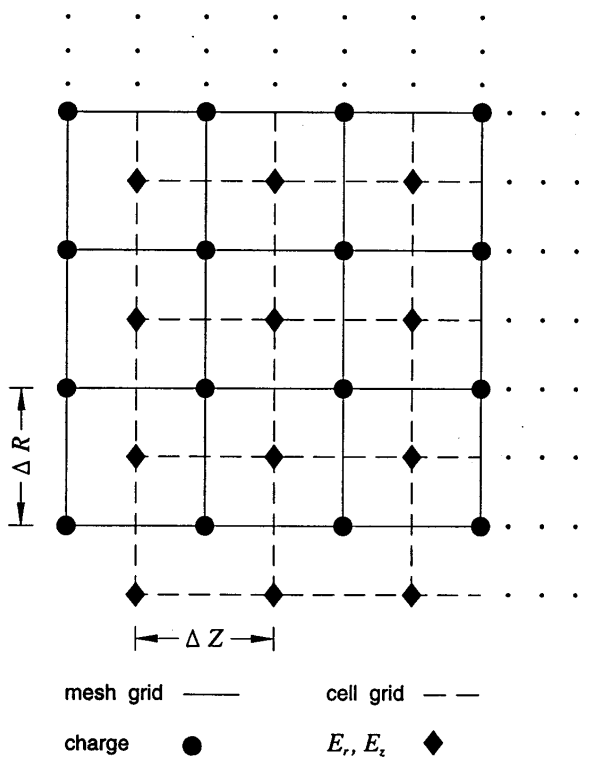

Space charge codes

4) assign macroparticle charges to mesh nodes, e.g. 1,2,3, and 4 vertices get QA_1/A, QA_2/A, QA_3/A, and QA_4/A respectively, where $A_1+A_2+A_3+A_4 = A = \Delta Z \Delta R$

5) calculate field at each cell by using mesh charges and table, e.g.
$\vec{E}(1), \vec{E}(2), \vec{E}(3), \vec{E}(4)$

6) find fields at macroparticle position by weighting
$(A_1\vec{E}(1) + A_2\vec{E}(2) + A_3\vec{E}(3) + A_4\vec{E}) / A$

7) Apply force to each macroparticle

8) Lorentz back-transform to the lab frame

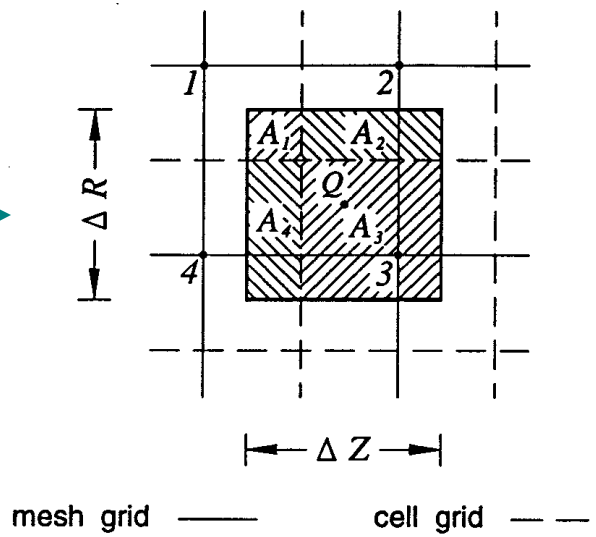

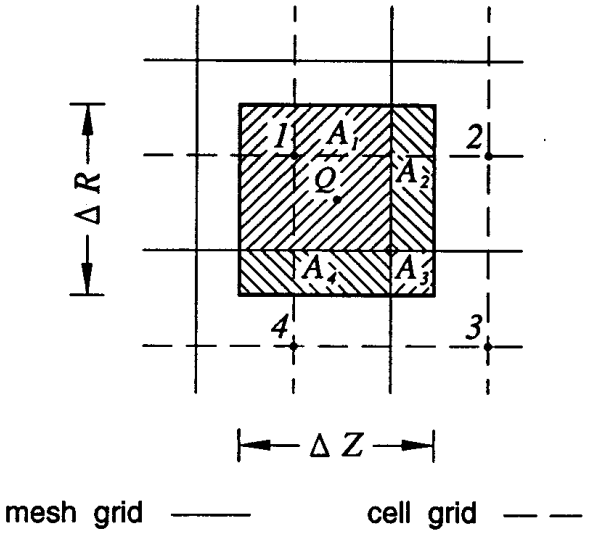

Common space charge code strategy

- Majority of injector design codes use the strategy:
  - Assume nearly monochromatic beam
  - Solve Poisson equation in the rest frame
    - various meshing strategies (simple uniform mesh for fast FFT methods, nonequidistant adaptive mesh for distributions with varying density)
    - Essentially removes granularity of the force
  - Lorentz back-transform and apply forces including 3D field maps of external elements (cavities, magnets, etc.)

Limitations

- Limitations of this method include:
  - Ignores interaction of charged beam with conducting walls of the chamber (wake fields; can be added ad hoc)
  - Fails if the beam has large energy spread
  - Most of the time removing excessive granularity from space charge is justified because the actual beam has many more particles than 'virtual' beam
  - However, the mesh method may lead to artificial 'over-smoothing' of the forces, underestimate intrabeam scat.
- There are powerful self-consistent Particle-In-Cell (PIC) codes. These require use of supercomputers.

Example of injector optimization

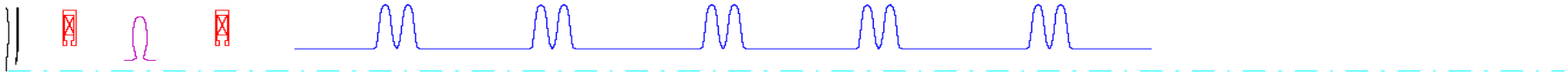

Fields:
DC Gun Voltage (300-900 kV)
2 Solenoids
Buncher
SRF Cavities Gradient (5-13 MV/m)
SRF Cavities Phase

Positions:
2 Solenoids
Buncher
Cryomodule

Bunch & Photocathode:
$E_{thermal}$
Charge

Laser Distribution:
Spot size
Pulse duration (10-30 ps rms)
{tail, dip, ellipticity} x 2

Total: 22-24 dimensional parameter space to explore

Example of beam dynamics: 80 pC charge

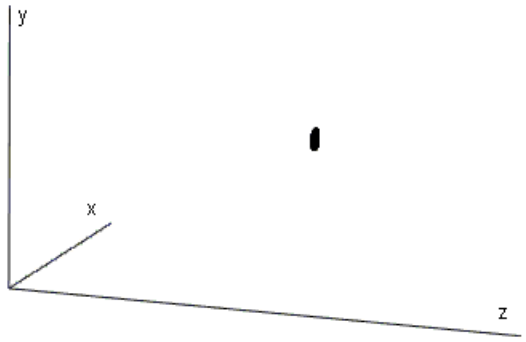

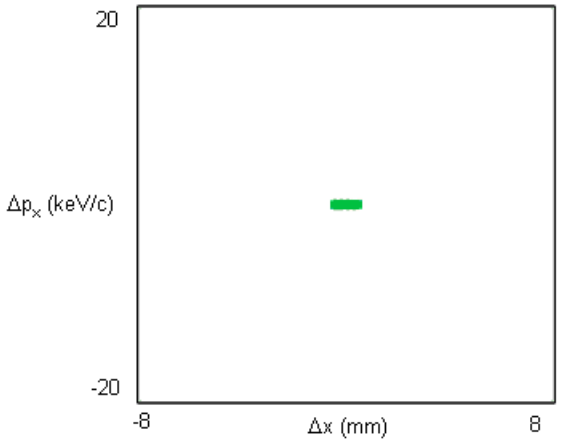

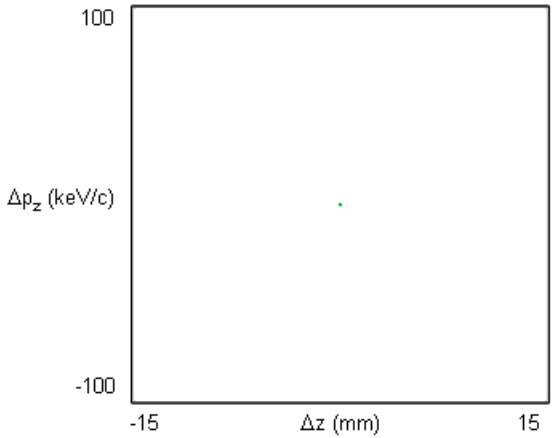

z = 0.000 m

p_z = 0.000 MeV/c

σ_x = 0.294	mm	ε_x = 0.077	mm-mrad
σ_z = 0.000	mm	ε_z = 0.000	mm-keV

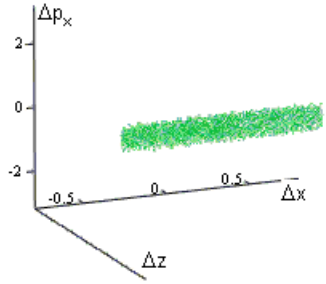

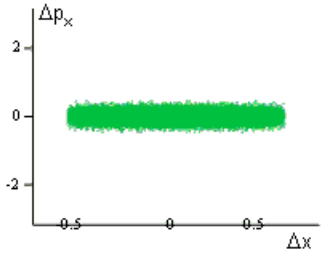

Example of beam dynamics: 0.8 nC charge

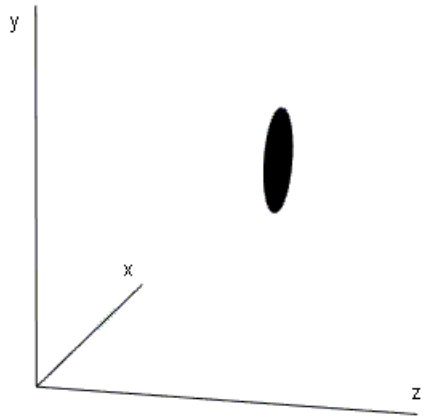

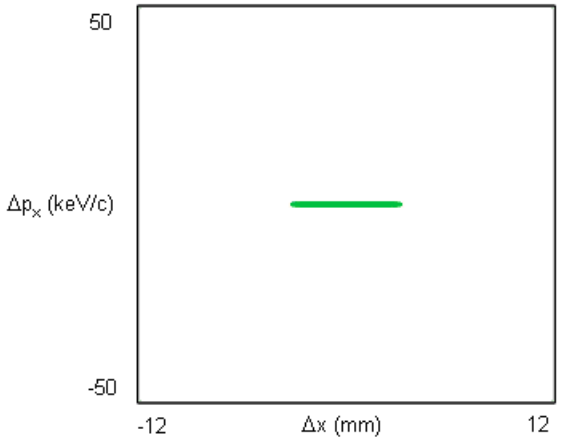

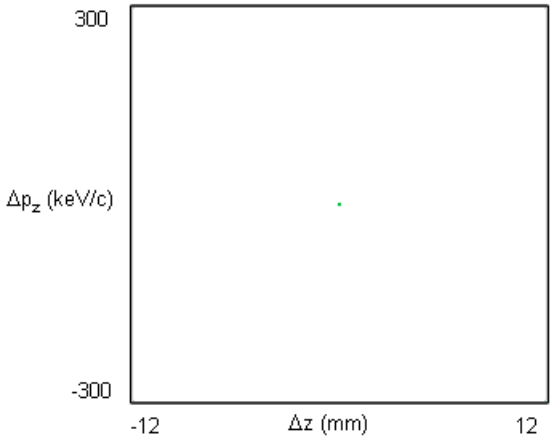

z = 0.000 m

p_z = 0.000 MeV/c

σ_x = 1.629 mm ε_x = 0.425 mm-mrad

σ_z = 0.000 mm ε_z = 0.000 mm-keV

Zoomed in transverse phase space

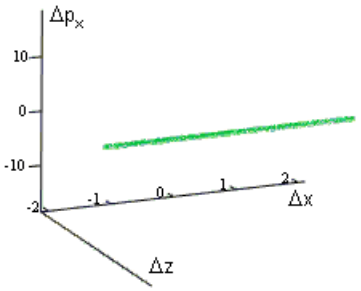

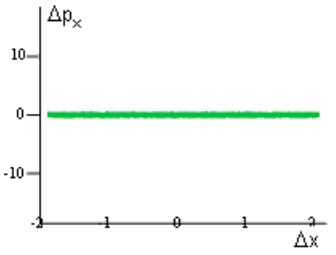

Injector performance

Takes several 10^5 simulations

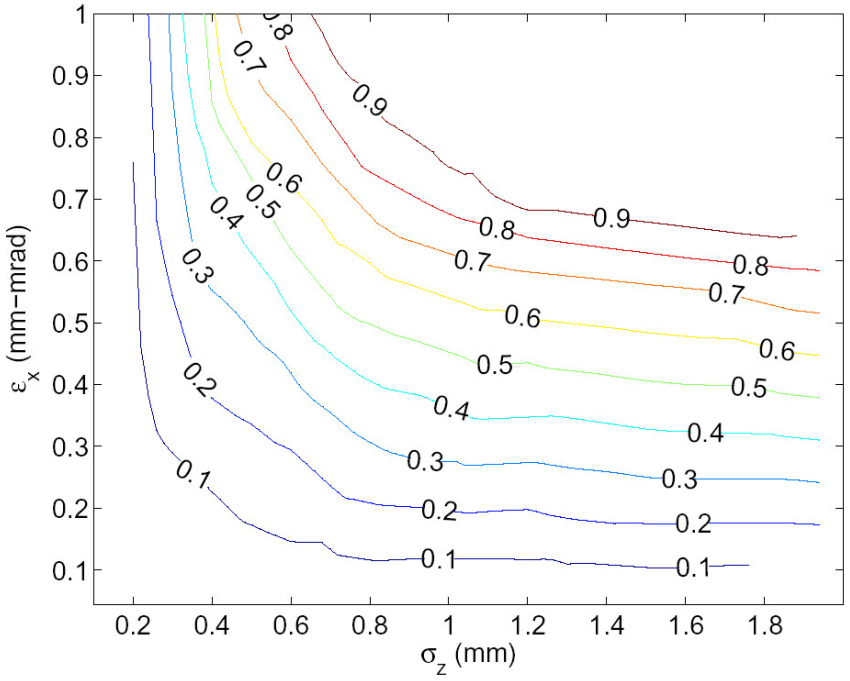

FIG. 10: Transverse emittance vs. bunch length for various charges in the injector (nC).

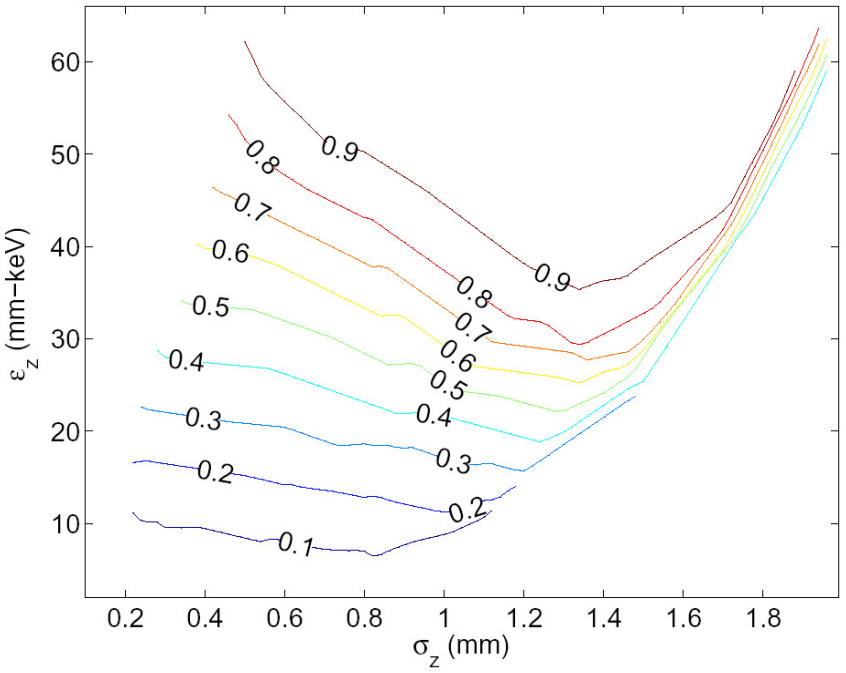

FIG. 11: Longitudinal emittance vs. bunch length for various charges in the injector (nC).

$$\varepsilon_n[\text{mm-mrad}] \approx (0.73+0.15/\sigma_z[\text{mm}]^{2.3}) \times q[\text{nC}]$$

Space charge basics

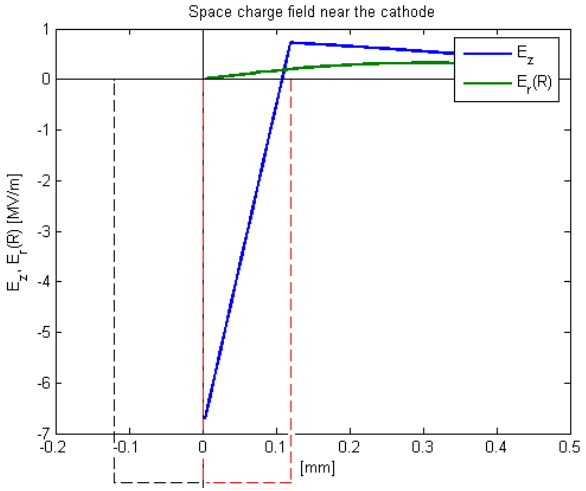

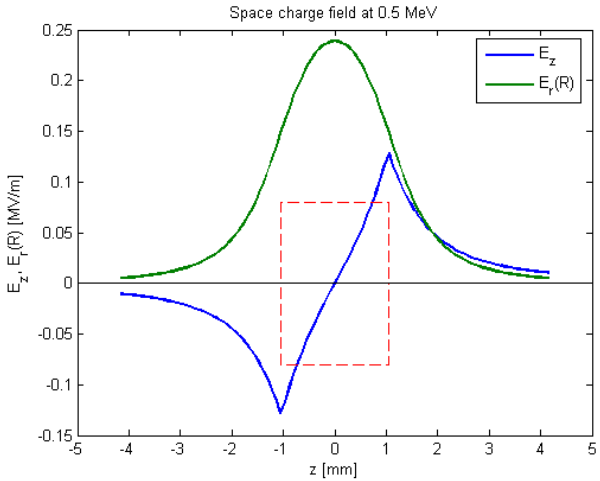

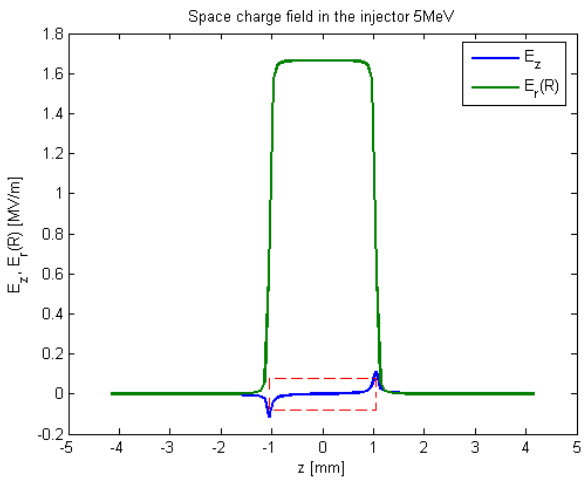

Beam envelope equation:

$$\ddot{R} + K_f R = \underbrace{\frac{e}{m\gamma}\left[E_r^{s.c.} - \beta c B_\theta^{s.c.}\right]} + \left(\frac{4\varepsilon_n^{th} c}{\gamma}\right)^2 \frac{1}{R^3}$$

$$\frac{e}{m\gamma^3} E_r^{s.c.}(R) = \frac{1}{2}\omega_p^2 R$$

$$\omega_p^2 = \frac{e^2 n}{\varepsilon_0 \gamma^3 m}$$

Beam temperature

Diffraction limited beam at 1Å → ε_x = 8pm at 5GeV → ε_{nx} = 0.08 μm

10 MV/m gradient → σ_{laser} = 0.3 mm

Transverse temp. needed ***kT = 25 meV***

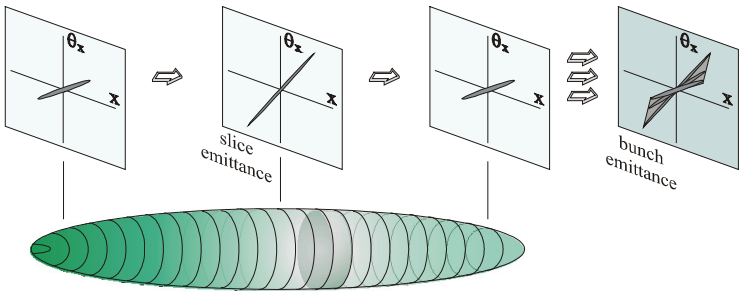

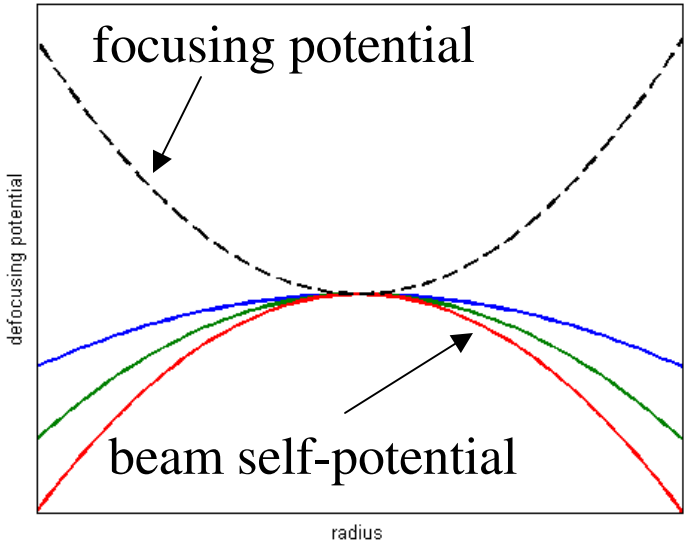

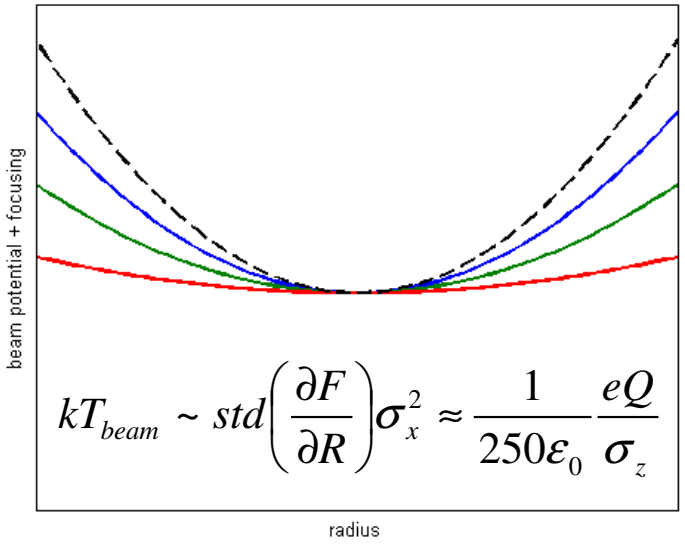

$$kT_{beam} \sim std\left(\frac{\partial F}{\partial R}\right)\sigma_x^2 \approx \frac{1}{250\varepsilon_0}\frac{eQ}{\sigma_z}$$

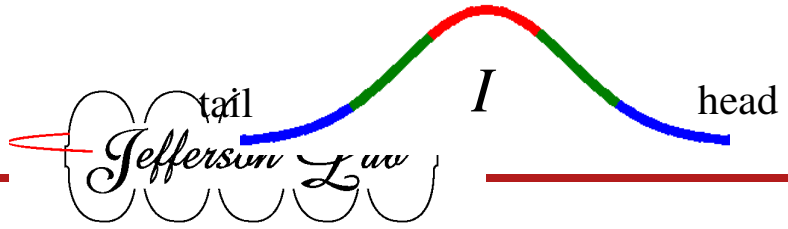

Equilibrium ***kT_{beam} ~ 100 eV!!***

Optimal initial (laser) distribution

If space charge force is linear within a bunch, there is no rms emittance growth associated with it. Uniform transverse distribution for cylindrical continuous beam is one example. For bunched beam, 3D ellipsoid satisfies the requirement

$$\frac{x^2}{A^2}+\frac{y^2}{B^2}+\frac{z^2}{C^2}=1, \quad \vec{E}=(E_x,E_y,E_z)=\frac{3q}{4\pi\varepsilon_0 ABC}(M_x x, M_y y, M_z z)$$

Under linear self-forces, the shape will remain to be elliptical. Luiten et. al suggested using elliptical 2D shape 'δ-function' laser pulse (~30 fs) to produce 3D ellipsoid under the influence of space charge near the cathode (PRL **93** (2004) 094802).

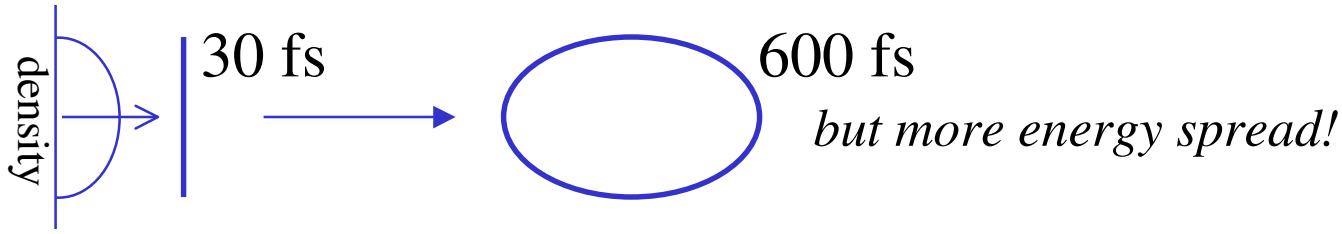

Optimal initial (laser) distribution

Several things change the idealistic 3D ellipsoid picture:

1) image charge at the cathode
2) distortion due to bunching

example for DC gun optimal shape (80 pC)

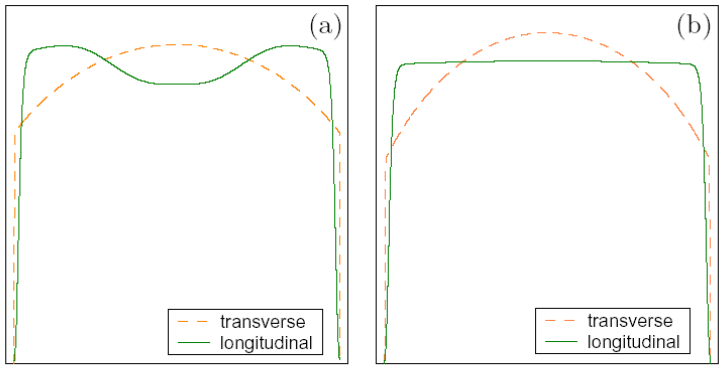

FIG. 6: Initial distribution profiles corresponding to minimal emittance at the end of the injector for (a) 80 pC and (b) 0.8 nC cases.

Phys. Rev. ST-AB **8** (2005) 034202

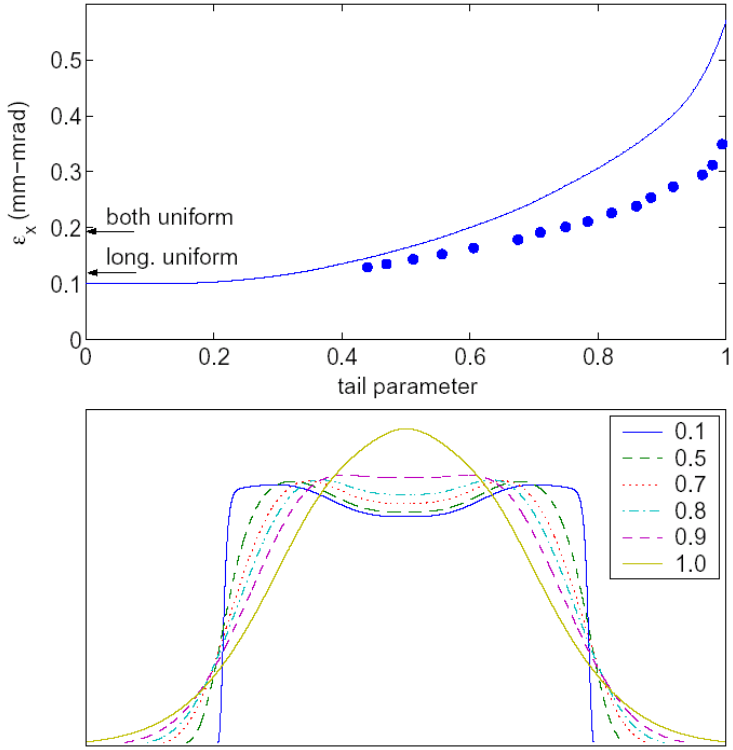

FIG. 7: 80 pC: emittance sensitivity (solid curve) to the longitudinal profile changes (top) and the corresponding profile shapes (bottom).